

Numerical Simulation of the Blast-Wave Accelerator

Dennis Wilson,* Zhiqiang Tan,[†] and Philip L. Varghese[‡]
 University of Texas at Austin, Austin, Texas 78712

A concept for propelling a projectile to hypervelocities is described, and the feasibility is demonstrated by numerical simulations. In theory, the concept employs imploding blast waves to accelerate a projectile as it travels down a launch tube. The launch tube can be open to the atmosphere or sealed and maintained at some low pressure to minimize internal drag. The launch tube has a liner that contains a suitable explosive or energetic material. The explosive is configured with inert annular rings to prevent upstream detonation. A suitable trigger detonates each explosive ring sequentially as the projectile passes. The resulting blast wave causes an elevated pressure on the afterbody of the projectile. The acceleration continues until the projectile exits the launch tube.

I. Introduction

THE blast-wave accelerator is a concept for propelling a projectile through a gun tube. The launcher concept and a preliminary quasisteady analysis was first presented at the first ram accelerator conference.¹ Multiple rings of explosives can be placed inside the wall of a standard gun tube, as shown in Fig. 1. The explosive rings are detonated sequentially by a mechanical or electromechanical trigger, and the resulting blast wave and subsequent high-pressure gas exert a force on the base of the projectile. The process can continue down the tube until the projectile reaches the desired velocity. The theoretical limiting velocity of the projectile can be very high. In the case of constant blast-wave velocity V_b and constant angle of the projectile afterbody with the tube axis α , this limiting velocity is $V_b/\sin \alpha$. In practice, V_b depends on the explosion intensity and the background pressure. It also varies spatially. However, a typical value is 10 km/s. For the geometry shown in Fig. 2 with $\alpha = 20$ deg, the limiting velocity is 29 km/s. In practice, the actual velocity would be considerably less. Note that the material strength of the projectile (and perhaps the tube if it is to be reusable) prohibits us from increasing the energy intensity arbitrarily along the tube.

In practice, the proposed design would probably be used to accelerate a projectile to hypervelocities using a conventional prelauncher such as a powder gun. The prelauncher would be used to accelerate a projectile to some modest velocity, say 1 km/s. The blast-wave accelerator then could be used to boost the velocity to much higher levels.

The blast-wave accelerator is energy efficient in terms of explosive mass consumed and gun tube length. The explosive is injected behind the projectile and thus is more efficient than traditional gun propulsion where the propellant is fixed at the breach end of the barrel. Indeed, the blast-wave accelerator is more like a rocket propelled inside a tube. In fact, the energy efficiency of the blast-wave accelerator is even higher than that of a rocket, because the fuel is not accelerated but, rather, it is fixed on the wall. By adjusting the explosive masses and positions, it is possible to achieve nearly optimal pressure distribution behind the projectile, so that the total acceleration is optimized.

The objective of this work is to investigate the projectile acceleration and flow behavior via numerical simulation. The analysis is intended to provide initial estimates of the launcher capabilities. In Sec. II, a literature review is presented. In Sec. III, the parameters of the simulated accelerator are given, and in Sec. IV the

governing equations are described. In Sec. V, the numerical procedure is described. In Sec. VI, the simulation of an idealized one-dimensional accelerator is presented, and in Sec. VII, the simulation of more realistic axisymmetric accelerators is described.

II. Literature Review

Background

Recently, the Space Systems Division at NASA Langley Research Center identified a national need for a launcher capable of accelerating large packages (nominal diameter of 250 mm, mass of 14 kg) to velocities of 6 km/s.² The proposed facility would be used primarily to study phenomena associated with hypervelocity aeroballistics and aerothermodynamics. The NASA study identified three existing technologies that have a reasonable probability for success: electromagnetic rail guns, ram/scram accelerators, and two-stage light gas guns. The ram/scram accelerator bears some similarity to the blast-wave accelerator. However, there is a fundamental difference in the operational principle.

The U.S. Army also has a strong interest in hypervelocity, high-energy launchers capable of accelerating masses of several kilograms to velocities in excess of 3 km/s.³ The primary motivation is to study large-scale hypervelocity impact and penetration dynamics. Other applications involve fundamental studies of material behavior at large strain rates, and development of extensive equation-of-state data.

More grandiose ideas such as impact fusion⁴ and low-Earth-orbit (LEO) insertion also have been suggested. Velocities in the 20-km/s

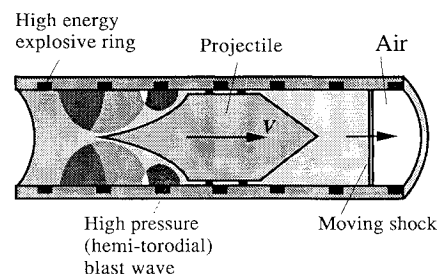


Fig. 1 Schematic of the blast-wave accelerator.

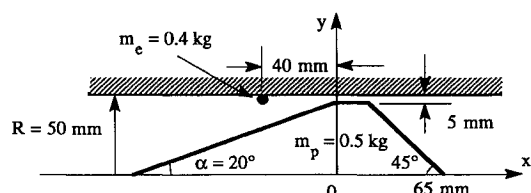


Fig. 2 Computational domain and coordinate system showing the axisymmetric accelerator model.

Presented as Paper 94-1994 at the AIAA 12th Applied Aerodynamics Conference, Colorado Springs, CO, June 20-23, 1994; received Sept. 26, 1994; revision received Dec. 27, 1995; accepted for publication Jan. 5, 1996. Copyright © 1996 by the American Institute of Aeronautics and Astronautics, Inc. All rights reserved.

*Associate Professor, Department of Mechanical Engineering. Senior Member AIAA.

[†]Postdoctoral Fellow, Institute for Advanced Technology. Member AIAA.

[‡]Associate Professor, Department of Aerospace Engineering and Engineering Mechanics. Senior Member AIAA.

regime are necessary to achieve impact fusion, whereas LEO insertion would require launch velocities approaching 10 km/s with masses of several hundred kilograms. Currently, no launcher exists for these regimes of the velocity/mass parameter space.

Explosive Launchers

During the past 30 years, there have been numerous designs proposed and prototype launchers built that employ an explosive to drive a projectile or a thin metal (flyer) plate at hypervelocities. For the purpose of this review, they are considered to fall into three broad categories: explosive guns, explosive shock tubes, and continuously detonated explosive launchers.

The simplest type of explosive launcher is the explosive gun. It is similar to a propellant gun, but contains a large quantity of high explosive (HE) in the breech. The HE is detonated and the resulting high-pressure gas is channeled into the barrel through a conical transition. The volume of the breech and conical transition region is typically equal to the barrel volume. The gun is usually designed for one shot because the operating pressure usually exceeds the material strength of the gun.

One of the first explosive guns built was described by Willig and Semon⁵ in 1959. It used 0.7 kg of composition C-4 explosive to accelerate a 6.35-mm-diam, 6.35-mm-long aluminum cylinder to 5.5 km/s. More recently, Holt et al.⁶ built a modified version of the explosive gun, which launched a 12.1-g steel projectile to 3.2 km/s using 0.82 kg of composition B explosive.

Explosive shock tubes convert HE energy into directional gas kinetic energy to produce shock-wave velocities of ~ 10 – 15 km/s in channels of relatively large cross sections ($\sim 10^2$ – 10^3 cm²). The conversion efficiency of HE into gas kinetic energy is approximately 10%. The earliest studies on the capabilities of explosive shock tubes date back to the mid-1950s. The first designs simply detonated a cylindrical HE inside a tube to produce a planar shock.⁷ More sophisticated designs, such as the Voitenko compressor,⁸ the shaped explosive driver,⁹ and the linear implosion driver,¹⁰ were developed during the 1960s. A discussion of the operational principle of these devices is given by Glass et al.,¹¹ who also describe an implosion-driven shock tube.

Finally, Menikoff et al.¹² studied a shock wave driven by a continuous phased implosion. The axially phased implosion on the wall of a channel acts as a virtual piston to drive a planar shock wave. Once again, their application was not a launcher but rather a system they described as a super shock tube.

Although these devices were developed for producing very-high-velocity and very-high-energy gas flows, there is no intrinsic problem in converting them into hypervelocity launchers. In fact, Titov and Fadeenko¹³ used an explosive-tube design to accelerate a small steel sphere by means of aerodynamic drag inside the shock tube.

Recently, experimental and computational work¹⁴ on plane-wave, explosive shock tubes designed to accelerate thin (1-mm) metal disks to velocities approaching 10 km/s has produced encouraging results. Three explosive launchers were studied. The first was a plane-wave shock tube (PWST). In this design, the disk is placed in contact with an explosive initiated by a plane-wave lens. The detonated gases expand behind the plate and accelerate it down the barrel. The fast shock tube (FST), similar in design, employs a plane-wave explosive lens. The detonation propagates a shock inside a cylinder containing a polystyrene foam, which acts like a gas. As the shock propagates in the foam, the Mach disk grows until it matches the diameter of the metal disk, which then is accelerated with a nearly planar pressure wave. The FST also can have a short barrel downstream of the thin disk, referred to as an FSTB, to confine the high-pressure gas and achieve higher velocities.

Marsh and Tan¹⁴ summarized the results of the experimental and computational effort on planar-wave explosive launchers at a recent conference on shock compression of condensed matter. They launched identical stainless-steel plates of 1.5-mm thickness and 11-mm diameter. The maximum, intact, plate velocities achieved for the PSWT, FST, and FSTB were 6.5, 7.4, and 9.0 km/s, respectively. Kerrisk and Meier¹⁵ addressed some of the problems associated with the FST. They noted that the peak pressure ranges from 30 to 100 GPa, which is well above any reasonable material strength

limit. Another problem is that during acceleration the driving gas pressure is not uniform over the plate.

The idea of using a tube lined with explosive to drive a projectile is not completely new. In fact, several concepts have been proposed that are quite similar to the blast-wave accelerator described in this paper. The Soviet literature contains two concepts that involve a continuously detonated explosive charge. Voitenko¹⁶ described a concept that he called the linear jet engine. The proposed design was a tube lined with a continuous layer of explosives. A projectile fired inside the tube would presumably detonate the explosive, which then would expand over the tail cone. No experiments or serious computations were reported. However, Voitenko made an estimate of the velocity using a simple, one-dimensional, quasisteady analysis. Based upon this analysis, he estimated a velocity of 8 km/s for a 1-kg projectile mass inside a 60-m-long tube containing 30 kg of explosives with an energy density of 4 MJ/kg. Another Russian concept similar to the previous one was proposed by Tatzhanov.¹⁷ The details for both the design and the analysis were very sketchy. Without presenting any justification, Tatzhanov claimed that a projectile of unspecified mass could reach a velocity of 8 km/s (the explosive detonation velocity) in a tube of unknown length. The explosive is detonated continuously in both of the designs; thus the detonation wave speed would strongly control the performance. The design proposed in this paper places discrete explosive rings along the gun tube, so that the charges can be detonated independently. This separates the projectile speed from the detonation wave speed, thus allowing precise control of the projectile acceleration inside the tube.

An explosive launcher very similar to the present design was described through a verbal communication with Dennis Bushnell,¹⁸ who visited the Central Research Institute of Machine-Building in Kalliningrad, Russia. During this visit, Pavel Kryukov described a launcher, referred to as a RAM mass accelerator. No sketches were available but, according to Bushnell, it was a tube with annular explosive charges. A single-page technical sheet listed the following information: length = 100 m, explosive mass = 150 kg, bore = 100 mm, projectile mass = 1.5–2.3 kg, injection velocity = 1.5 km/s, and expected muzzle velocity = 9 km/s. The project status was described as follows: accelerator model has been built; synchronous ignition of high explosives has been experimentally confirmed; experiments to define ignition delay time have been performed. The authors are not aware of any further information or experiments.

Hertzberg et al.¹⁹ have suggested an HE-driven ram accelerator that is similar to the blast-wave accelerator. In this design, the projectile is injected down a tube that contains a continuous HE coating between a thin metal liner and the gun tube. The normal shock on the rear of the projectile is assumed to produce a pressure high enough to detonate the HE, which then drives the metal liner inward to choke the flow, thus maintaining the shock on the aft end of the projectile. The authors claim that this will then produce a self-synchronized operation mode. They also estimate that velocities of 20–30 km/s are theoretically possible. Finally, Cambier and Bogdanoff²⁰ suggested firing a subcaliber projectile inside a tube and using the oblique shock to detonate an explosive on the tube wall.

Propellant Launchers

There are several propellant-type launchers that apply either a discrete or a continuous impulse along the length of the launch tube. The earliest design involved a traveling-charge concept or impulse gun originally proposed by Langweiler.²¹ More recently, experiments at the Ballistic Research Laboratory (now the Army Research Laboratory) have produced muzzle velocities in excess of 2 km/s for a charge-to-projectile mass ratio of 1.6.²² In a traveling-charge gun, fast-burning propellant is attached to the base of a projectile. The projectile is launched by a conventional gun and the traveling charge ignites after a slight delay so as to increase the down-bore base pressure on the projectile.

Another design that involves a discrete distribution of powder charges along the gun tube, known as the Hochdruckpumpe, was built by the Germans during World War II.²³

A more recent design, which bears a strong resemblance to the blast-wave accelerator but is quite different in its operational principle, is the ram/scram accelerator. Work on the ram accelerator has

been carried out for over 10 years primarily at the University of Washington, the Army Research Laboratory, and the Institut Saint Louis. The ram/scram accelerator is based upon the ramjet principle. A projectile that resembles the centerbody of a ramjet travels down the center of a tube filled with a premixed gaseous fuel and an oxidizer. The basic principle involves an energy release process due to combustion. The resulting high pressure acts on the aft portion of the projectile in a continuous manner as it travels down the tube. The blast-wave accelerator is fundamentally different in that an explosive on the tube wall is detonated and the resulting blast wave exerts a high pressure on the aft end of the projectile. The design and operation of the ram/scram accelerator are discussed in Ref. 24. According to that study, the authors claim that velocities of ~ 0.7 to ~ 12 km/s and masses from grams to hundreds of kilograms are possible. The range is achieved by five basic modes of ram acceleration operation. There are two subsonic combustion modes, a normal overdriven detonation mode, and two oblique detonation modes. To date, experimentally demonstrated velocities have been limited to approximately 2.7 km/s. Finally, Rodenberger et al.²⁵ conducted a feasibility study on an accelerator concept that employed a thin layer of propellant lining a gun barrel as the major energy source. This concept is similar to the proposed blast-wave accelerator.

III. Mathematical Model

In all of the numerical simulations, we assume that the length of the gun tube is infinite ($-\infty < x < +\infty$). A fixed domain is used to solve the moving-boundary problem by fixing the coordinate system on the projectile (Fig. 2). The detonation of the explosion is assumed to be instantaneous and the volumes of the explosives are extremely small, so that the energy and mass releases from the detonations can be modeled as point sources or sheet sources for the one-dimensional accelerator example. The masses of the projectile and the explosive are denoted as m_p and m_e , respectively. The axial spacing between explosive charges is l_e and the energy density e is 5 MJ/kg in all of the calculations.

For simplicity, we assume that the flow is axisymmetric and the detonation products and the surrounding gas are perfect and inviscid. The specific-heat ratio γ is 1.4 everywhere. We are only interested in fluid dynamic and thermodynamic behaviors; therefore, the barrel and the projectile are assumed to be rigid and no material response is considered. In addition, there is no friction between the barrel and the projectile. By computing the flowfield around the projectile, we can simulate the movement of the projectile from the surface pressure and Newton's second law. The gas is initially at rest and has a density of 1 kg/m^3 and a pressure of 10^5 Pa .

If serious consideration were to be given to constructing a laboratory prototype launcher, several refinements in the analysis would need to be made. Most notably, the material properties of the launcher and the projectile would need to be considered.

IV. Governing Equations

Because the geometry surrounding the projectile is unchanged at all times, we can fix the computational coordinate system on the projectile with the origin $x = 0$ at the left shoulder (see Fig. 2). The Euler equations are

$$w_t + f_x + g_y + s_1 + s_2 = 0 \quad (1)$$

where

$$w = \begin{bmatrix} \rho \\ \rho u \\ \rho v \\ e \end{bmatrix}, \quad f = \begin{bmatrix} \rho u \\ \rho u^2 + p \\ \rho uv \\ \rho u H \end{bmatrix}, \quad g = \begin{bmatrix} \rho v \\ \rho uv \\ \rho v^2 + p \\ \rho v H \end{bmatrix}$$

and ρ is the density, u and v are the velocities, e is the total energy, p is the pressure, and H is the total enthalpy.

The source terms are defined as

$$s_1 = \frac{\rho v}{y} \begin{bmatrix} 1 \\ u \\ v \\ H \end{bmatrix} \quad \text{and} \quad s_2 = \rho \begin{bmatrix} 0 \\ h \\ 0 \\ hu \end{bmatrix} \quad (2)$$

where $h = \dot{V}$ is the acceleration of a flow particle due to the non-inertial motion of the reference frame, and V is the traveling speed of the projectile. The term s_1 is due to axisymmetry, and the term s_2 accounts for the effect of the noninertial reference frame.

Writing the speed V and position X of the projectile in the lab coordinate system, the equations governing $V(t)$ and $X(t)$ are given by Newton's second law as

$$m_p \dot{V} = \int_{\Gamma_p} p(r, t) n_x d\Gamma, \quad \dot{X} = V(t) \quad (3)$$

with initial conditions

$$V(0) = 0, \quad X(0) = 0$$

where Γ_p is the boundary of the projectile, n_x is the x component of the inward normal of Γ_p (i.e., the outward normal of the gas boundary), and p is the pressure on Γ_p .

The explosions are idealized as point mass and energy source releases: the total mass M and energy E of the explosive product is added to the gas in a very small area surrounding the point of detonation.

V. Numerical Method

A time-splitting method is applied to Eqs. (1) to separate the sourceless Euler equations from the source terms. This makes it possible to use an existing Euler code without modifications.

The sourceless Euler equations are

$$w_t + \nabla \cdot \mathbf{F} = 0 \quad (4)$$

where $\mathbf{F} = (f, g)^T$. The finite element equations can be obtained by the usual Galerkin procedure:

$$L_i w_{it} - \sum_{e=1}^{N_e} \int_{\Omega_e} \mathbf{F} \cdot \nabla \phi_i^e d\Omega + \text{boundary terms} = 0 \quad (5)$$

where ϕ_i^e is the shape function in element e , N_e is the element number, and L_i is the lumped mass. Quadrilateral elements are used with upwind flux calculations. The method was developed in Ref. 26, and some improvements have been made. These are outlined below. In this scheme, the integral in Eq. (5) is first approximated by

$$\begin{aligned} & - \int_{\Omega_e} \mathbf{F} \cdot \nabla \phi_i^e d\Omega \frac{1}{8} [(I_3 + I_4 - I_1 - I_2) \cdot (\mathbf{F}_1 + \mathbf{F}_2) \\ & - (I_2 + I_3 - I_4 - I_1) \cdot (\mathbf{F}_4 + \mathbf{F}_1)] \equiv \frac{1}{4} |I_3 + I_4 - I_1 - I_2| \\ & \cdot \mathbf{n}_{i2} \cdot \mathbf{F}_{i2} - \frac{1}{4} |I_2 + I_3 - I_4 - I_1| \mathbf{n}_{i4} \cdot \mathbf{F}_{i4} \end{aligned} \quad (6)$$

when i is the first node of element e and $\mathbf{I} \equiv (-y, x)^T$ and $\mathbf{F}_{ab} = (\mathbf{F}_a + \mathbf{F}_b)/2$. The approximation when i is any other node of e can be written similarly. Then, an upwind scheme is used to calculate the fluxes $\mathbf{n} \cdot \mathbf{F}$. In our work, the Harten-Lex-van Leer-modified method²⁷ is applied. This method's performance is similar to that of Roe's method but requires no entropy corrections. Second-order accuracy is obtained by applying a modified van Albada flux limiter.²⁸ For time stepping, a simple first-order explicit scheme is used.

The term s_1 is treated by a partially implicit scheme when $v^+ < 0$ and explicitly when $v^+ \geq 0$:

$$\begin{aligned} \frac{w^{(n+1)} - w^+}{\Delta t} &= \frac{\rho^{(n+1)} v^+}{y} \begin{bmatrix} 1 \\ u \\ v \\ H \end{bmatrix}^{n+1} & \text{when } v^+ < 0 \\ &= s_1^+ & \text{when } v^+ \geq 0 \end{aligned}$$

The terms with superscript $+$ are the results from the sourceless Euler step. This approach allows for a less restricted Courant-Friedrichs-Lewy number. After s_1 is accounted for, the noninertial term s_2 is then advanced in time with first-order forward time stepping.

After the Euler equations (1) are integrated, the body motion equation (3) is solved. Traditionally, the pressure computed from the Euler equations would be used to calculate the force term on the right-hand side of Eq. (3). However, it was found that better results with improved stability can be achieved through the solution of the mass-damped Riemann problem.²⁹ Thus the star pressure p^* of the approximate solution of the mass-damped Riemann problem is used. This pressure is given by

$$p^*(r) \equiv p(r)s\left(\sqrt{\gamma}\frac{v \cdot n - V}{a}\right) \quad (7)$$

Here, s is defined by

$$s(x) = \begin{cases} 1 + (x^2/2)\left\{\gamma_+ + [\gamma_+^2 + (4\gamma/x^2)]^{\frac{1}{2}}\right\} & x \geq 0 \\ \left\{\max[0, 1 + (\gamma_-/\sqrt{\gamma})x]\right\}^{\gamma/\gamma_-} & x < 0 \end{cases} \quad (8)$$

with $\gamma_{\pm} \equiv (\gamma + 1)/2$. The details of the mass-damped Riemann problem are given in Ref. 29. Because Eq. (7) is now a function of V , an implicit scheme can be used to advance Eq. (3) in time. This increases the stability of the calculation when the impulse from the explosion is high.

The detonation source term is approximated by a piecewise linear distribution, with high values of density and pressure being added to the state at the node of explosion. The values are calculated from the total mass and energy of the explosion.

The code has been used to calculate several benchmark problems, including the one-dimensional piston motion driven by a strong shock. The results are in good agreement with analytical or approximate solutions. Details are given in Ref. 29.

VI. One-Dimensional Ideal Blast-Wave Accelerator Simulation

Model Description

To test the code, an idealized one-dimensional model is first solved. This is done by replacing the projectile with a piston, and detonating the explosives behind the piston as it travels down the tube.

The tube diameter is 0.1 m, the piston diameter is 0.09 m, and the mass is 0.5 kg. The gas is initially static, and the projectile is at rest. In this idealized model, a 0.4-kg sheet explosive is detonated at 0.04 m behind the base. As the projectile travels through the gun barrel, 70 more explosives are sequentially detonated at the same position relative to the projectile, when the projectile center passes the 0.1-, 0.2-, ..., 7.0-m marks in the lab coordinate system. The energy density of the explosives is 5 MJ/kg.

Numerical Results

The computational domain is confined to $-0.2 < x < 0.1$ and $0 < y < 0.05$ m in the projectile coordinate system, with $x = 0$ on the base and $y = 0$ on the symmetry axis. About 5700 nodes, which are nearly uniformly distributed in the computational domain, are used in the computation.

The traveling speed and force distribution for the first 10 explosions are shown in Fig. 3a. The results for all 71 explosions are shown Fig. 3b. The delay in the arrival time of each successive blast wave, clearly visible in Fig. 3a, is the result of two effects. First, the projectile is accelerating away from the blast wave, and second, the blast-wave velocity is decreasing because of the higher background density in which the blast wave is propagating. The peak force of the later blasts also decreases because of two effects. First, as the projectile velocity increases, the blast-wave velocity relative to the projectile decreases; thus the interaction between the blast wave and the projectile is reduced. Another cause is the cushion effect, which is discussed below in the numerical results for model 1.

As the projectile speed increases, the efficiency decreases dramatically. The maximum speed in this case is limited by the blast-wave speed. From Fig. 3b, we expect that a speed higher than 7 km/s would be very difficult to obtain in practice.

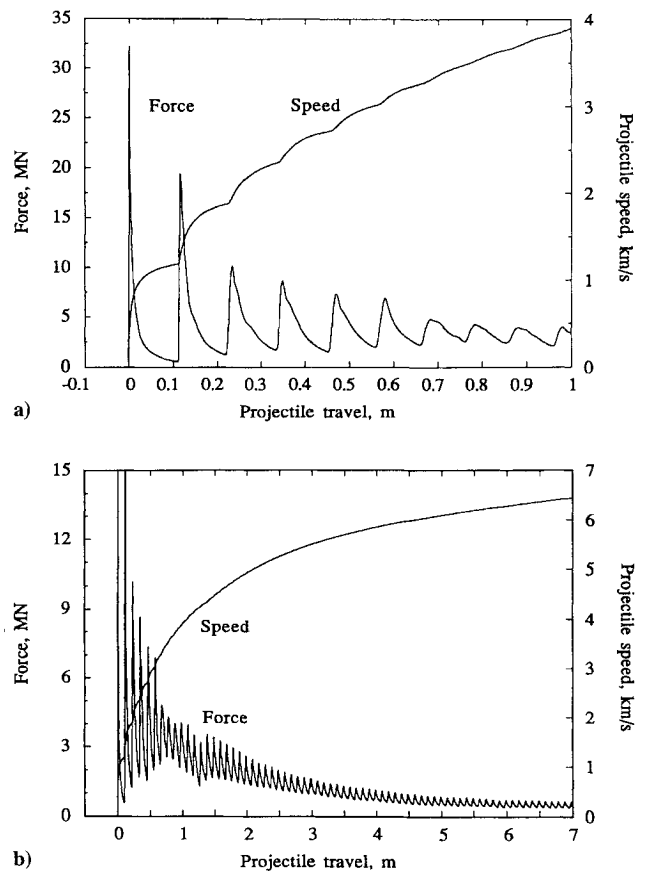


Fig. 3 Force and traveling-speed history for the one-dimensional accelerator: a) first 10 blasts and b) all 71 blasts.

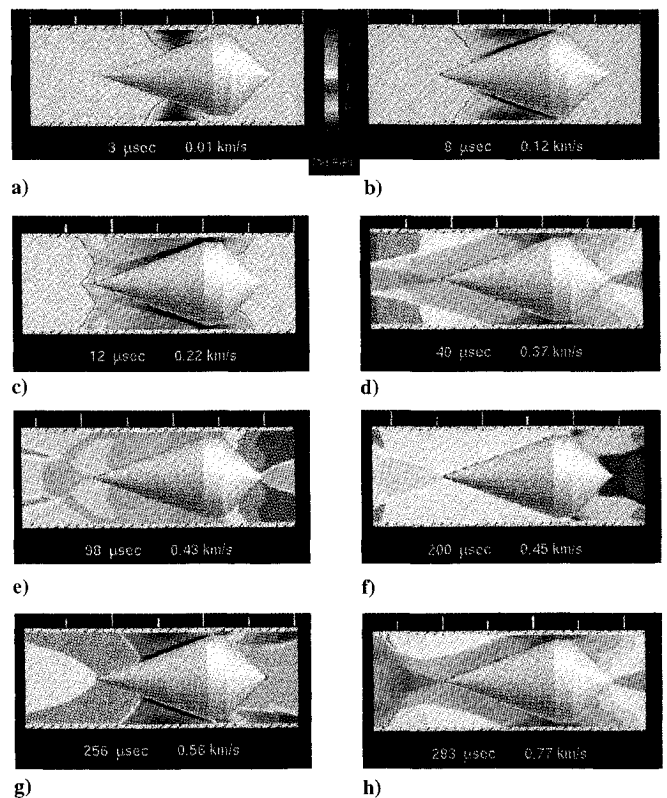


Fig. 4 Numerical simulation a conceptual blast-wave accelerator. The projectile is accelerated by 71 stages of blasts to 7 km/s. Pressure profile and traveling speed of the projectile are shown. Note the movement of the projectile relative to the lab coordinate system. Only the early two stages are shown.

Analytical Approximation

Certain features of the numerical solution can be explained by exploiting analytical results from classic blast-wave theory.³⁰ For the case of a planar blast wave, the shock velocity obeys the following relation in the early stages following detonation:

$$V_s = \frac{2}{3}[(E/A)/\rho_0]^{\frac{1}{2}}(1/x^{\frac{1}{2}}) \quad (9)$$

In this equation, ρ_0 is the background density, E is a constant related to the total energy release of the explosive, and A is the area. In the approximate theory, the energy release occurs instantaneously and has zero volume. This, of course, gives a singularity in both space and time. Nevertheless, the analytical theory is quite useful for providing insight into propagational behavior of blast waves.

In classic blast-wave theory, the background pressure p_0 is negligible relative to p_s , and the initial gas velocity is zero. This results in the following expression for the shock pressure p_s :

$$p_s = [2/(\gamma + 1)]\rho_0 V_s^2 \{1 - [(\gamma - 1)/2\gamma](a_0^2/V_s^2)\} \quad (10)$$

If we use these equations for the early acceleration stages and use the strong shock approximation, we find that

$$p_s = \frac{8}{9}[(E/A)/(\gamma + 1)](1/x) \quad (11)$$

When the shock strikes the piston, the pressure increase at the surface is approximately $2\gamma/(\gamma - 1)$. For subsequent reflections, the pressure increase will be less. Also, after the shock strikes the piston, this simple $1/x$ decay law no longer applies. However, if we ignore these complexities, then the following equation of motion for the piston can be written:

$$m_p V_p = \frac{dV_p}{dx} = \frac{8}{9} \frac{E}{\gamma + 1} \frac{1}{x} \quad (12)$$

If we let $E = \frac{1}{2}$ of the total energy release (one-half of the energy travels in the negative x direction) and integrate over one pulse from l_d to $l_d + l_e$, we obtain

$$V_p = \left[\frac{8}{9} \frac{m_e}{m_p} e^{\frac{l_e}{l_d} [1 + (l_e/l_d)]} \frac{1}{\gamma + 1} \right]^{\frac{1}{2}} \quad (13)$$

Using $e = 5$ MJ/kg, $l_d = 0.04$ m, and $l_e = 0.1$ m, we find the piston velocity after one detonation to be 1.36 and after 11 detonations we obtain 4.52 km/s. The corresponding numerical simulation gives 1.18 and 3.9 km/s, respectively. In spite of the gross approximations, the analytical results are in good agreement with numerical computations over the first 11 detonations. The simple analytical solution demonstrates the expected trend, namely that the velocity is proportional to the square root of the charge-to-projectile mass ratio.

A final result from the approximate theory helps to explain the limiting velocity of the ideal one-dimensional acceleration. From Eq. (9), we can write the velocity at the piston surface as

$$V_s = \frac{2}{3}[(E/A)/\rho_0]^{\frac{1}{2}}(1/\Delta x^{\frac{1}{2}}) \quad (14)$$

We can obtain an estimate of ρ_0 from conservation of mass by writing

$$\frac{1}{2}\rho_e h_e A = \rho_0 A \Delta x_e \quad (15)$$

where Δx_e is the distance between explosive charges and h_e is the total thickness of the charge. For $\rho_e = 1.5 \times 10^3$ kg/m³, this gives a limiting background density of 20 kg/m³. Using this value in Eq. (14), we find a limiting shock velocity of 8.4 km/s. The numerical simulation show an asymptotic value that appears to approach this value.

VII. Axisymmetric Blast-Wave Simulation

The maximum limiting speed achievable in the one-dimensional case does not imply that the two-dimensional accelerator also is limited by this speed. As discussed above, for the accelerator shown in Fig. 2, if the angle α between the base and the tube is small, the projectile speed V can be significantly higher than the blast-wave speed V_b . Assuming that V_b is constant, a simple calculation gives $V_{\max} = V_b/\sin \alpha \gg V_b$ for small α .

Two numerical simulations were conducted. The first is the axisymmetric analog to the one-dimensional ideal accelerator and the second is a geometry representative of a proposed experiment.

Model 1 Description

The geometric and physical parameters and the computational parameters of the two-dimensional axisymmetric simulation are shown in Fig. 2. The projectile and explosive mass are the same as the one-dimensional ideal accelerator. The afterbody angle is 20 deg, and the forebody angle is 45 deg. The explosive is detonated at 0.04 m behind the rear shoulder of the projectile and 2.5 mm from the tube wall. The energy density of the explosive is still 5 MJ/kg, and again, 71 explosions of 0.4-kg charges are used.

Numerical Results

Figure 4 shows the flowfield of the first two explosions. The resolution of the detonation waves is quite sharp, as seen from Fig. 5. (Note that a logarithmic scale is used in the plot.)

In the classic similarity theory for blast waves, the mass of the explosion product is ignored. The result is that the pressure is low in the center region of the blast wave. However, in numerical simulations, the explosive mass of each charge is much higher than the mass of the gas in the neighborhood of the explosion. The inertia of the dense explosion products prevents fast conversion of the internal energy to kinetic energy. A thin layer of very dense, high-pressure gas is found near the wall during the early stages of each explosion. This is because the explosive is placed at a distance (2.5 mm) from the wall. The pressure increases after a reflection. The reflection is clearly seen to cause a kink in Fig. 4a. The main part of the blast wave in Fig. 4a is not circular. This is due to blast-wave implosion in the radial direction and explosion along the tube axis.

The blast is reflected back after it hits the base of the projectile Fig. 4b. The high-energy explosion products near the barrel continue to expand and force the reflected gas from the projectile to form a layer of hot, dense gas that covers the entire base. This layer moves backward relative to the projectile eventually forming a jet at the end of the projectile (Figs. 4c–4g).

This hot and dense gas layer also acts as a cushion against the blast waves from later explosions. Figures 5a and 5b show the projectile traveling speed and the force. The peaks of the later explosions become less sharp, indicating that the blast waves have been damped. This cushion effect, a result of damping of the pressure peaks, can be beneficial for practical designs where the material response must be considered.

The calculations show that the distribution of the explosion products is very favorable in that most of the high-pressure region is on the base of the projectile. Some explosion gases leak into the front side of the projectile for the subcaliber projectile used in this numerical simulation. The amount is very small and the resulting force is negligible compared to the back side. The projectile for a real accelerator will be full caliber or have a much smaller annular gap than the one used in the simulation. The subcaliber geometry was used in the numerical simulation to avoid a sharp corner in the computational domain that may have negative effects on accuracy and numerical stability. Note that even when there is no leakage, the pressure in the right region will increase with traveling speed, because the shock-induced pressure in front of the projectile will continually increase. Figure 6 shows the projectile speed as a function of time.

The arrival times of the blast waves are nearly the same for all explosions. This is different from the one-dimensional case and is expected. The delay in arrival time would be significant only when V is close to $V_{\max} = V_s/\sin \alpha$. The average blast-wave speed calculated from the numerical simulations is approximately 10 km/s. Therefore, for $\alpha = 20$ deg, $V_{\max} \approx 29$ km/s, which is much higher

than the maximum projectile speed of approximately 7 km/s in the one-dimensional accelerator.

The force on the projectile becomes smaller in the later stages, as shown in Fig. 5. As traveling speed increases, the distance traveled during the time between detonation and blast arrival also increases. This shifts the pressure peak on the projectile base toward the rear, where the circumference is smaller, thus reducing the net force. The cushion effect also reduces the pressure peak. One way to increase the force for the later stages would be to detonate the explosives earlier, so that the blast can arrive at the same position on the projectile base. Although the final velocities for both one- and two-dimensional simulations are almost the same, the degeneration in efficiency when projectile speed is large is much smaller in the two-dimensional case than the one-dimensional case. This is easily seen by comparing Fig. 3b with Fig. 4b.

The pressure plots for the first two explosions (Figs. 4a–4h) show that the maximum pressure on the projectile base rarely exceeds 1 GPa, which is within the strength limit of many materials. The peak pressures are much smaller for later explosions. In an optimal design, smaller charges would be used for earlier explosions so that the peak pressures stay the same for all explosions.

Another simulation was conducted using much higher charge-to-projectile mass ratio. Similar trends were found but are not shown here. Grid convergence was performed in this simulation using two different grid sizes. The difference between the results was small.

Model 2 Description

To date, no experiments have been conducted, but a simple proof of concept experiment has been proposed. A circular cylinder with a flat base is prelaunched at 1.3 km/s into a gun tube. A series of explosive rings along the tube wall will detonate as the projectile passes. The tube diameter is 10 cm, and the explosive ring detonates when the projectile base is 0.04 m from the charge. Other parameters are as follows: a) the projectile is full caliber, b) the mass of the projectile is 90 g, c) each charge has a mass of 10 g, d) the initial

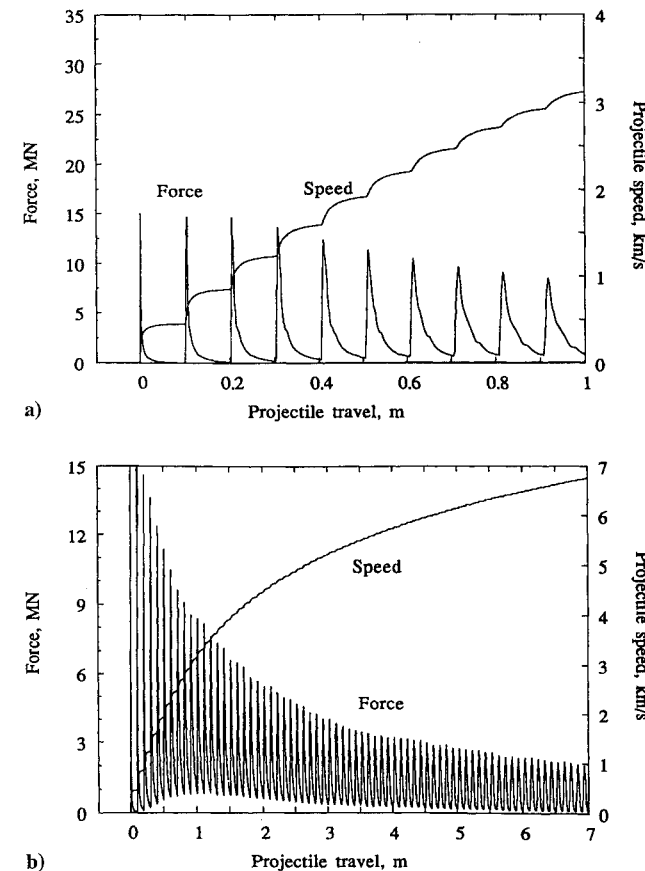


Fig. 5 Force and traveling-speed history of the axisymmetric accelerator: a) first 10 blasts and b) all 71 blasts.

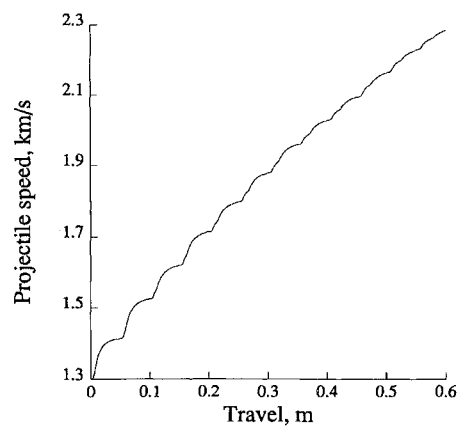


Fig. 6 Traveling speed for the low-charge accelerator.

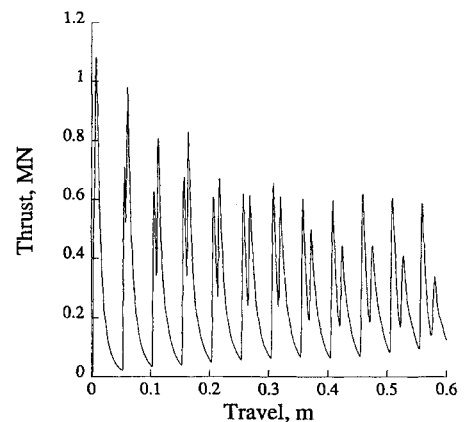


Fig. 7 Thrust for the low-charge accelerator.

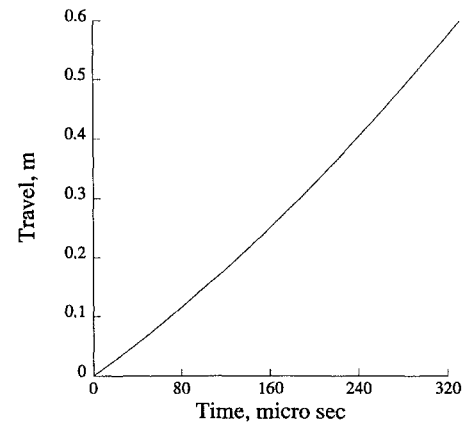


Fig. 8 Trajectory of the low-charge accelerator.

projectile velocity is obtained by another mechanism, and e) there are 12 explosives. The same energy density of 5 MJ/kg is used.

Numerical Results

The speed, thrust, and trajectory are shown in Figs. 6, 7, and 8, respectively. Because the overall projectile speed is low, the degradation in energy efficiency for subsequent detonations is quite small. Because of the lower energy density, the peak pressure on the projectile is 1 GPa, roughly at the limit of high-strength steels. Despite the low energy density, the acceleration is very large, about 300,000 g, and the energy efficiency is about 30%, which is very high.

The first peak in the force (thrust) in Fig. 7 is due to the initial impact of the blast wave on the projectile. The second peak visible for

detonations 2–12 is due to a high-pressure jet along the centerline, which was observed in pressure contours. As the shock waves converge along the centerline of the tube, an extremely high pressure occurs. This produces a nearly cylindrical virtual shock tube along the launch-tube centerline. Its diameter was approximately 20% of the launch-tube diameter. The effect is similar to the so-called super shock tube described in Ref. 12. This phenomenon has interesting possibilities for producing a super shock tube using phased annular ring explosions.

Approximate Analysis

We can again exploit the ideal-blast-wave theory to find the projectile velocity as a function of the accelerator parameters. If we assume a cylindrical line charge of length πD and energy E , then the shock pressure can be written as

$$p_s = \frac{1}{2}[(E/\pi D)/(\gamma + 1)](1/r^2)$$

where r is the distance from the explosive line charge. If we take r as the tube radius ($D/2$), then an approximate expression for the peak force on the cylinder is

$$F_x = \frac{1}{2}[(E/D)/(\gamma + 1)]$$

From this result, we find that the projectile velocity after $i + 1$ detonations can be written as

$$V_{p,i+1} = \{V_{p,i}^2 + (m_e/m_p)e[(\Delta l/D)/(\gamma + 1)]\}^{\frac{1}{2}}$$

where Δl is the distance between each charge. Using an insertion velocity of 1.3 km/s, we find the final velocity after 12 detonations to be 2.22 km/s, which is remarkably close to the numerical solution of 2.28 km/s.

VIII. Conclusions

Our calculations show that, in theory, the blast-wave accelerator can accelerate projectiles to very high speeds (7 km/s for the present model). By tuning the shape and increasing the total charge, much higher speeds can be achieved. The distribution of the high-pressure gas is favorable, in that most of it surrounds the rear of the projectile. For the axisymmetric accelerator simulation, about 8% of the chemical energy is converted into the kinetic energy of the projectile. This is a satisfactory efficiency for a hypervelocity launcher. At lower speed, the efficiency is even higher. Previous calculations using a quasisteady analysis indicate that by modifying the geometry and explosive parameters, higher efficiencies can be achieved.

The present simulations are still preliminary. We have yet to explore the parameter space by considering different charge distributions, different projectile shapes, and different detonating strategies. However, the exploration should be straightforward with the numerical model established in this paper. Future modification on the numerical model will include nonperfect gas effects and chemical reactions.

Acknowledgments

Financial support was provided by the Institute for Advanced Technology, under U.S. Army ARDEC Contract DAAA 21-93-C-0101. The computation resources were provided in part by the University of Texas System Center for High Performance Computing and the Pittsburgh Supercomputing Center.

References

- Wilson, D., "Blast Wave Accelerator," Ram Accelerator Conf., Institut Saint Louis, France, Sept. 1993.
- Witcofski, R., Scallion, W., and Carter, D., "Advanced Hypervelocity Aerophysics Facility: A Ground Based Flight Test Range," AIAA Paper 91-0296, Jan. 1991.
- Reinecke, W. G., and Legner, H. H., "Review of Hypervelocity Projectile Aerophysics," AIAA Paper 95-1853, April 1995.
- Winterberg, F., "Magnetic Booster Target Low Velocity High Yield

Impact Fusion," *IEEE Transactions on Magnetics*, Vol. MAG-18, No. 1, 1982, pp. 213–216.

⁵Willig, F. J., and Semon, H. W., "Multi-Stage Actuated Hypervelocity Gun," *Proceedings of the 3rd Symposium on Hypervelocity Impact*, Vol. 1, Armour Research Foundation, Illinois Inst. of Technology, Chicago, IL, 1959.

⁶Holt, W. H., Soper, W. G., and Mock, W., "Explosive Gun Launcher for Impact Studies," *International Journal of Impact Engineering*, Vol. 5, No. 3, 1987, pp. 357–362.

⁷Schreffler, R. G., and Christian, R. H., "Boundary Disturbance in High-Explosive Shock Tubes," *Journal of Applied Physics*, Vol. 25, No. 2, 1954, pp. 324–331.

⁸Voitenko, A. E., "Generation of High Speed Gas Jets," *Soviet Physics—Doklady*, Vol. 9, No. 11, 1965, pp. 860–862.

⁹Cowan, M., "Ionizing Shocks from High Explosives," Sandia Lab., SC-RR-69-320, Albuquerque, NM, 1969.

¹⁰Gill, S. P., and Goettelman, R. C., "Implosively Accelerated Shock Tube Driver," NASA CR-950, Nov. 1967.

¹¹Glass, I. I., Chan, S. K., and Brode, H. E., "Strong Planar Shock Waves Generated by Explosively Driven Spherical Implosions," *AIAA Journal*, Vol. 12, No. 3, 1974, pp. 367–374.

¹²Menikoff, R., Lackner, K. S., Johnson, N. L., Colgate, S. A., Hyman, J. M., and Miranda, G. A., "Shock Wave Driven by a Phased Implosion," *Physics of Fluids*, Vol. A3, No. 1, 1991, pp. 201–218.

¹³Titov, V. M., and Fadeenko, Y. I., "Acceleration of Solid Bodies by Cumulative Explosions," 2nd International Colloquium on Gasdynamics of Explosions and Reactive Systems, Novosibirsk, USSR, 1969.

¹⁴Marsh, S. P., and Tan, T.-H., "Hypervelocity Plate Acceleration," Los Alamos National Lab., LA-UR-91-2001, Los Alamos, NM, 1991.

¹⁵Kerrisk, J. F., and Meier, J. K., "Problems Associated with Launching Hypervelocity Projectiles from the Fast Shock Tube," Los Alamos National Lab., LA-UR-92-1529, Los Alamos, NM, 1992.

¹⁶Voitenko, A. E., "Principal Energy Characteristics of a Linear Jet Engine," *Journal of Applied Mechanics and Technical Physics* (USSR), Vol. 31, No. 2, 1990, pp. 273–275.

¹⁷Tatshanzov, V. I., "Massive Body Acceleration on the Detonation Wave Front," *Combustion, Explosion and Shock Waves* (USSR), Vol. 27, No. 2, 1991, pp. 130–132.

¹⁸Bushnell, D., private communication, NASA Langley Research Center, Hampton, VA, 1993.

¹⁹Hertzberg, A., Bruckner, A. P., and Mattick, A. T., "Chemical Method for Achieving Acceleration of Macroparticles to Ultrahigh Velocities," Final Rept., Aerospace and Energetics Research Program, Univ. of Washington, Seattle, WA, April 1987.

²⁰Cambier, J.-L., and Bogdanoff, D. W., "RAM Acceleration from a Two-Phase Detonative System," Ram Accelerator Conf., Institut Saint Louis, France, Sept. 1993.

²¹Langweiler, H., "A Proposal for Increasing the Performance of Weapons by the Correct Burning of Propellant," British Intelligence Objective Subcommittee, Group 2, Ft. Halstead Exploiting Center, England, UK, 1940.

²²Oberle, W. F., III, White, K. J., Tompkins, R. E., and Juhasz, A. A., "Traveling Charge Computations—Experimental Comparisons and Sensitivity Studies," U.S. Army Ballistic Research Lab., Rept. BRL-TR-2844, Aberdeen Proving Ground, MD, Aug. 1987.

²³Hogg, I. V., *The Illustrated Encyclopedia of Artillery*, Chartwell Books, 1987, p. 167.

²⁴Hertzberg, A., Bruckner, A. P., and Bogdanoff, D. W., "Ram Accelerator: A New Chemical Method for Accelerating Projectiles to Ultrahigh Velocities," *AIAA Journal*, Vol. 26, No. 2, 1988, pp. 195–203.

²⁵Rodenberger, C. A., Sawyer, M. L., and Tower, M. M., "On the Feasibility of Obtaining Hypervelocity Acceleration Using Propellant Lined Launch Tubes," NASA CR 108699, Oct. 1970.

²⁶Tan, Z., and Varghese, P. L., "Directionally Adaptive Finite Element Method for Multidimensional Euler and Navier–Stokes Equations," AIAA Paper 93-3320, July 1993.

²⁷Einfeldt, B., Munz, C. D., Roe, P. L., and Sjogreen, B., "On Godunov-Type Methods near Low Densities," *Journal of Computational Physics*, Vol. 92, No. 2, 1991, pp. 273–295.

²⁸Van Albada, G. D., van Leer, B., and Roberts, W. W., "Comparative Study of Computational Methods in Cosmic Gas Dynamics," *Astronomy and Astrophysics*, Vol. 108, No. 1, 1982, pp. 76–84.

²⁹Tan, Z., Wilson, D., and Varghese, P. L., "Mass-Damped Riemann Problem and the Aerodynamic Surface Force Calculation for an Accelerating Body," *Journal of Computational Physics* (to be published).

³⁰Sedov, L. I., *Similarity and Dimensional Methods in Mechanics*, Academic, New York, 1959.